

Near-Infrared Spectroscopy for Measuring Urea in Hemodialysis Fluids

CHRISTOPHER V. EDDY AND MARK A. ARNOLD*

Background: Near-infrared spectroscopy is proposed as a method for providing real-time urea concentrations during hemodialysis treatments. The feasibility of such noninvasive urea measurements is evaluated in undiluted dialysate fluid.

Methods: Near-infrared spectra were collected from calibration solutions of urea prepared in dialysate fluid. Spectra were collected over three distinct spectral regions, and partial least-squares calibration models were optimized and compared for each. Selectivity for urea was demonstrated with two-component samples composed of urea and glucose in the dialysate matrix. The clinical significance of this approach was assessed by measuring urea in real hemodialysate samples.

Results: Urea absorptions within the combination and short-wavelength, near-infrared spectral regions provided sufficient spectral information for sound calibration models in the dialysate matrix. The combination spectral region had SEs of calibration (SEC) and prediction (SEP) of 0.38 mmol/L and 0.26 mmol/L, respectively, over the 4720–4600 cm^{-1} spectral range with 5 partial least-square factors. A second calibration model was established over the combination region from a series of solutions prepared with independently variable concentrations of urea and glucose. The best calibration model for urea in the presence of variable glucose concentrations had a SEC of 0.6 mmol/L and a SEP of 0.4 mmol/L for a 5-factor model over the 4600–4350 cm^{-1} spectral range. There was no significant decrease in SEP when the 4720–4600 cm^{-1} calibration model was used to measure urea in real samples collected during actual hemodialysis.

Conclusions: Urea can be determined with sufficient sensitivity and selectivity for clinical measurements within the matrix of the hemodialysis fluid.

© 2001 American Association for Clinical Chemistry

Hemodialysis is a clinical procedure for removing toxic substances from the blood of individuals with severe renal dysfunction. In this procedure, arterial blood is continuously removed from the patient through an implanted fistula. Low-molecular weight toxins are removed by dialysis by passing across a dialysis membrane from the blood to a recipient, dialysate fluid. The treated blood then returns to the body. Typically, each dialysis treatment requires 3–5 h and must be preformed every 3–4 days.

The effectiveness of a dialysis treatment is judged by the extent to which toxins are removed from the overall systemic pool of blood. Blood urea concentrations are commonly used as a measure of blood toxicity both between and during treatments. The period and frequency of hemodialysis treatments (i.e., the dialysis dosage) must be established individually for each patient. Various factors can change the effectiveness of a given dialysis dosage, including diet, physical activity, residual urea clearance, and fistula efficiency. Variations in these factors demand periodic (monthly or quarterly) reassessment of the dialysis dosage for each patient. The process is further complicated by an apparent discrepancy between the removal of toxins in the dialyzed blood and the retention of toxins in the systemic blood (1, 2). A two-pool blood model has been proposed to account for this confounding factor (3).

Continuous, “on-line” monitoring of the urea removed during dialysis is recognized as a first step toward improving treatment efficiency (4, 5). Several reports have detailed urea biosensors designed to measure urea accumulation in the recipient dialysis stream during treatment. Two basic approaches are reported. Each involves the catalytic conversion of urea to ammonium and bicarbonate ions by immobilized urease. The extent of urea hydrolysis by urease is determined either by a change in solution conductivity or by measuring the ammonium ion activity with an ion-selective membrane electrode (6–9).

In general, near-infrared (NIR)¹ spectroscopy offers an alternative approach for clinical analyses. In this ap-

Department of Chemistry and Optical Science and Technology Center, University of Iowa, Iowa City, IA 52242.

*Author for correspondence. Fax 319-335-1115; e-mail mark-arnold@uiowa.edu.

Received March 26, 2001; accepted April 10, 2001.

¹ Nonstandard abbreviations: NIR, near infrared; sw-NIR, short-wavelength NIR; PLS, partial least square; SEC, SE of calibration; SEP, SE of prediction; MPE, mean percentage of error; RMS, root mean square; μAU , microabsorbance units; SDC, SD of calibration; and SDP, SD of prediction.

proach, a selected band of near-infrared light is transmitted through the sample, and the analyte concentration is obtained by analysis of the resulting spectral information. This approach is nondestructive and reagentless, thereby permitting subsequent analyses. In addition, information for multiple analytes can be obtained from a single NIR spectrum (10, 11). Complex biological samples have been measured by NIR spectroscopy. Examples include the measurement of protein, cholesterol, urea, and glucose in undiluted samples of human serum (12) and the noninvasive measurement of glucose in human subjects with diabetes (13, 14).

We were interested in assessing the analytical utility of NIR spectroscopy for measuring urea in spent dialysate fluid. In this investigation, the three major regions of the NIR spectrum were evaluated for the selective measurement of urea in the basic matrix of the dialysate solution. The best analytical performance corresponded to measurements within the combination spectral range, which extended from 5000 to 4000 cm^{-1} (2.0–2.5 μm). The accuracy of these urea measurements was further demonstrated by measuring urea in a set of calibration solutions composed of independent concentrations of urea and glucose dissolved in the dialysate fluid. The ability to measure glucose in these calibration solutions was also established.

Materials and Methods

EXPERIMENTAL APPARATUS

Combination spectra (5000–4000 cm^{-1}) were collected with a Nicolet Magna 550 Fourier transform infrared spectrometer (Nicolet Analytical Instruments). This spectrometer was equipped with a standard 20-watt tungsten source, a calcium-fluoride beam splitter, and a cryogenically cooled indium antimonide (InSb) detector. Detection was restricted to the combination spectral region by positioning an interference filter (2.0–2.5 μm ; Barr and Associates, Inc.) immediately before the sample.

First overtone spectra (6500–5500 cm^{-1}) and short-wavelength NIR (sw-NIR) spectra (12 500–8600 cm^{-1}) were collected with a modified Nicolet 740 spectrometer. This spectrometer was equipped with a 400-watt tungsten lamp enclosed in a water-cooled housing equipped with a back-reflector mirror. For first overtone spectra, the spectrometer was configured with a calcium fluoride beam splitter, a room-temperature indium gallium arsenide detector, a 1.49 μm long-pass filter, and a 1.85 μm short-pass filter. These filters were positioned before the sample to restrict the spectral measurement to the first overtone range and to avoid heating the samples. For sw-NIR spectra, the spectrometer was configured with a quartz beam splitter, a silicon detector, and an LG-750-S filter positioned after the sample. A 30% transmittance, neutral-density filter was also required for the sw-NIR spectra to avoid detector saturation.

MATERIALS

Urea, glucose, and 5-fluorouracil were obtained from Sigma. Solutions were prepared gravimetrically in a commercially available bicarbonate-buffered dialysate solution (Cobe-Gambro-Hospal). The stock dialysate solution was diluted to an appropriate volume by staff in the Dialysis Clinic at the University of Iowa Hospitals and Clinics. The dialysate solution contained glucose (11 mmol/L), acetic acid (3 mmol/L), and the following chloride salts: potassium (2 mmol/L), sodium (135 mmol/L), calcium (7 mmol/L), and magnesium (2 mmol/L). The antimicrobial agent 5-fluorouracil (0.4 mg/g) was added to retard bacterial contamination and maintain solution integrity throughout.

PROCEDURES

Spectra were collected in triplicate without moving the sample between spectra. Samples were held in a thermostated Wilmad sample holder equipped with sapphire windows (diameter, 25 mm). Solution temperature was maintained at a targeted value by circulating temperature-controlled water from a VWR model 1140 water bath (VWR Scientific). Temperature during data acquisition was monitored with a copper-constantine thermocouple probe [diameter, 0.08 mm (1/32-inch); Omega Inc.] positioned in the circulating water bath. Samples were preheated in a separate water bath before injection into the sample cell. A 5-min period was permitted to allow thermal equilibration before data collection. The order of spectra collection was random with respect to analyte concentration to avoid temporal correlations within the data set (15).

Teflon spacers were used to control the optical pathlengths of the sample cells. The pathlength was 1.5 mm for the combination spectra and 10.0 mm for both the first overtone and sw-NIR spectra. Sample cells were assembled carefully to ensure that no portion of the Teflon spacer was in the optical path. Solution temperatures were maintained at 37, 38, and 35 °C for combination, first overtone, and sw-NIR spectra, respectively.

Spectra were collected as 256 coadded, 16-kilobyte, double-sided interferograms. Fourier processing led to single-beam spectra with 2 cm^{-1} point spacing. All single-beam spectra were processed with an Iris Indigo computer (Silicon Graphics Inc.). All spectral processing was accomplished using software tools provided by Professor Gary W. Small from the Center for Intelligent Chemical Instrumentation in the Department of Chemistry at Ohio University (Athens, OH).

Multivariate calibration models were constructed using the partial least-squares (PLS) algorithm (16, 17). Models were developed using a previously described optimization procedure (11). Briefly, each full data set was split into separate calibration and prediction data sets. The prediction data corresponded to all replicate spectra collected from 10 randomly selected samples. The remaining calibration data were divided into separate

training and monitoring data sets. The monitoring data set consisted of all spectra associated with 10 randomly selected samples from the calibration data set. Three unique splittings of the calibration data set were used to establish the optimum parameters for calibration. Once obtained, the optimized parameters were applied to the full calibration data set to establish the final calibration model. Model performance was evaluated by comparing the SE of calibration (SEC), the SE of prediction (SEP), and the mean percentage of error (MPE). These values of interest are defined elsewhere (11).

Real hemodialysis samples were collected from the effluent drain of five different machines during actual hemodialysis treatments at the University of Iowa Hospitals and Clinics. The urea concentrations in these samples were measured by the urease/Berthelot reaction scheme (18), and the measured values were 1.98, 3.88, 6.29, 10.73, and 15.67 mmol/L. NIR spectra were collected in triplicate over the combination region with the Nicolet Magna 550 FTIR spectrometer as described above. Single-beam spectra were collected from solutions maintained at 37 ± 0.1 °C, and reference spectra corresponded to blank unexposed dialysate fluid.

Results

The full NIR spectrum extends from 14 285 to 4000 cm^{-1} (0.7–2.5 μm). Three major water absorption bands are present within this range. These bands are centered at 3750, 5200, and 6950 cm^{-1} , and a smaller band exists at 8600 cm^{-1} . These strong water absorption bands effectively divide the full NIR spectrum into three distinct spectral windows. The chemical information within the combination range (5000–4000 cm^{-1}) corresponds to the combination of bending and stretching vibrations associated with CH, NH, and OH molecular groups. Information in the first overtone range (6500–5500 cm^{-1}) originates from the first overtone of stretching vibrations of CH and OH groups. Absorption features in the sw-NIR range (12 500–8600 cm^{-1}) correspond to higher order overtones and combinations associated with CH, NH, and OH moieties.

COMBINATION NIR SPECTRA

The two large water absorption bands centered at 5200 cm^{-1} and 3750 cm^{-1} define the combination spectral range. The absorbance spectrum of urea over this spectral range is presented in Fig. 1. This spectrum reveals two broad absorption bands centered at 4650 cm^{-1} and 4550 cm^{-1} . These bands correspond to the combination of the symmetric (~ 3350 cm^{-1}) and asymmetric (~ 3450 cm^{-1}) N–H stretching bands coupled with the N–H bending vibration (~ 1640 – 1600 cm^{-1}) (19). Hydrogen bonding in the aqueous environment causes a red shift in vibrational frequencies (20). The magnitude of this red shift is ~ 400 cm^{-1} for the combination bands of urea, a shift that is consistent with previous reports for amides in aqueous media (21).

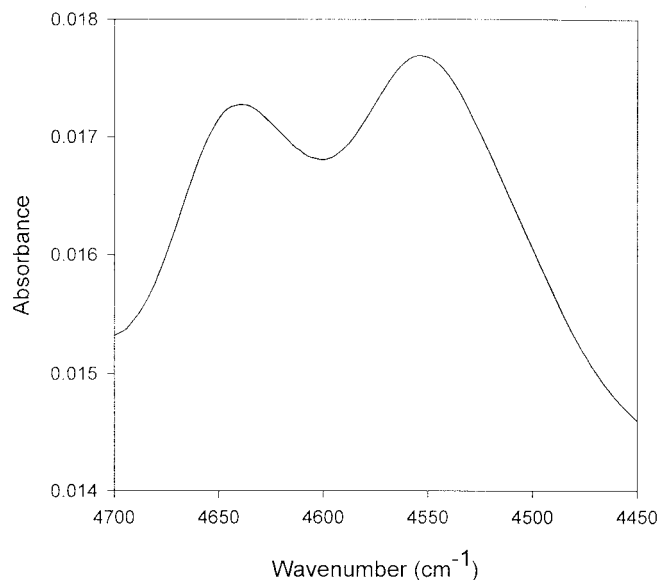


Fig. 1. Absorbance spectrum of 32 mmol/L urea in the dialysate matrix.

The analytical utility of the combination region was established by evaluating calibration models from combination spectra collected from a series of urea calibration solutions. These solutions were prepared by dissolving known amounts of solid urea in specific volumes of the dialysate fluid. The urea concentrations were 1–36 mmol/L for these 84 independent samples. A total of 252 spectra were collected. Unfortunately, one spectrum for three of these samples was inadvertently lost. As a result, a total of 249 spectra were stored and used to build the PLS calibration models for urea.

The quality of these spectra was established by computing the root mean square (RMS) noise for 100% lines. As detailed elsewhere (22), the 100% lines were computed by dividing the first spectrum by the second spectrum for each sample. The resulting 100% lines were converted to absorbance units and then separated into 10 discrete, 100- cm^{-1} increments (e.g., 5000–4900 cm^{-1} , 4900–4800 cm^{-1} , and so forth). The data across each segment were fitted to a second-order polynomial, and the RMS noise was computed. The results of these measurements are summarized in Table 1. This table lists the mean RMS noise value computed across all 84 of the urea calibration solutions for each segment. As noted previously (22), the lowest noise is obtained in the center of this spectral range and is consistent with the overall transmission properties of these aqueous samples. Mean RMS noise of 2.15–3.30 microabsorbance units (μAU) characterize these spectra over the spectral range that contains the urea-specific information (4700–4400 cm^{-1}).

PLS calibration models were constructed by processing raw single-beam spectra without normalization, mean centering, windowing, or digital filtering. An optimum model was established by considering the spectral range and the number of latent variables (factors or rank) by a

Table 1. RMS noise on 100% lines for combination spectra collected from urea calibrators in the dialysate matrix.

Segment, cm^{-1}	5000–4900	4900–4800	4800–4700	4700–4600	4600–4500
RMS noise, μAU	2100	105	10.5	3.26	2.15
Segment, cm^{-1}	4500–4400	4400–4300	4300–4200	4200–4100	4100–4000
RMS noise, μAU	2.51	6.14	45.9	889	5100

procedure detailed elsewhere (11). The best analytical performance was obtained with a 5-factor model over the 4720–4600 cm^{-1} spectral range. This range encompasses only the high-frequency absorption band of urea (see Fig. 1). A concentration correlation plot is presented in Fig. 2 for this optimized calibration model. Both the calibration and prediction data fall along the unity line. An analysis of residuals indicated no systematic deviation from this unity line as a function of urea concentration. For these data, the SEC, SEP, and MPE were 0.38 mmol/L, 0.26 mmol/L, and 2.2%, respectively.

FIRST OVERTONE NIR SPECTRA

Urea has no significant absorption features in the first overtone spectral range. The first overtones of the asymmetric and symmetric N–H stretches for urea are buried under the 6950 cm^{-1} absorption band of water. Nevertheless, the ability to measure urea in this spectral region was explored. The aim of this experiment was to establish the impact of water displacement on PLS calibration models of this nature. For calibration solutions composed of urea dissolved in buffer or dialysate, a correlation exists be-

tween the concentration of urea and the amount of water displaced by this urea. Higher concentrations of urea correspond to less water for a given volume of solution. Usually this relationship between solute and solvent is negligible and can be ignored. The strong absorption of NIR light by water, however, opens the possibility of measuring solute concentration through solvent displacement effects. If the solute concentration is correlated with the amount of solvent in the sample and the amount of solvent in the sample alters the spectrum in a systematic manner, then functional PLS calibration models can be constructed for the solute. Essentially, the solvent-induced spectral variations are used to predict solute concentrations through this concentration correlation. The absence of a significant absorption feature for urea in the first overtone spectral region provides an excellent opportunity to evaluate the impact of solvent displacement on model performance.

A series of urea calibration solutions was prepared as described above. In this experiment, 79 unique calibration solutions were prepared with a urea concentration range of 1–32 mmol/L. First overtone spectra were collected in triplicate and in random order with respect to urea concentration. As before, PLS calibration models were built using raw single-beam spectra, and spectral quality was measured as the RMS noise on 100% lines.

Results of the RMS noise measurements are summarized in Table 2. In this table, the mean values are reported for all 79 samples. As expected, the lowest RMS noise is observed in the center of this full spectral range, where the transmission of water is highest (11).

An optimized PLS calibration model was determined as before. The best analytical performance was achieved with a 4-factor model over a spectral range of 6090–5800 cm^{-1} . This spectral range corresponded to the low-noise portion of the spectra as is indicated by the results tabulated in Table 2. The SEC, SEP, and MPE values for this model were 7.63 mmol/L, 6.71 mmol/L, and 42%, respectively. These values of SEC and SEP essentially matched the SD of the urea concentrations in the calibration and prediction data sets, respectively. The SDs of urea concentration in the calibration (SDC) and prediction (SDP) data sets were 7.9 and 7.6 mmol/L, respectively. The strong similarity between SEC and SDC and between SEP and SDP values is a strong indication that the PLS model is incapable of predicting urea concentration from the input spectra. We conclude from this finding that the degree of water displacement in these urea calibration solutions is insufficient for modeling urea concentration.

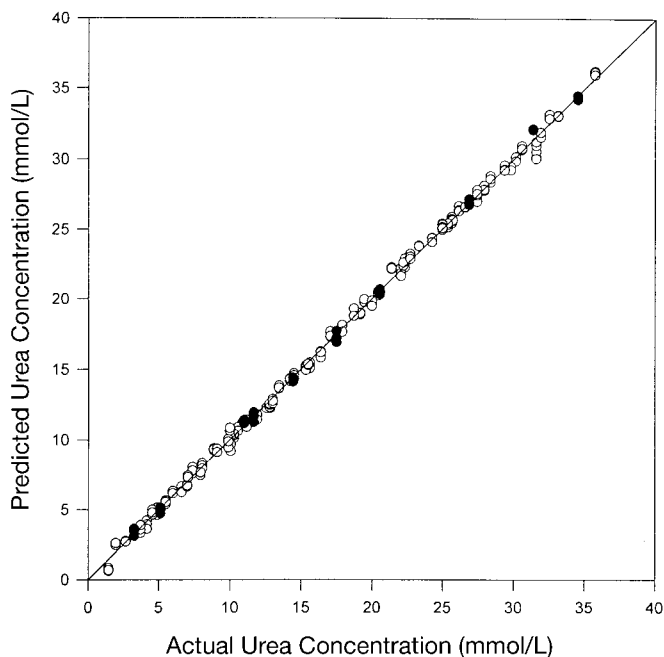


Fig. 2. Concentration correlation plot for urea in the 5000–4000 cm^{-1} spectral range.

Open circles are the calibration data, and filled circles are the prediction data. The optimum calibration model was built over the 4720–4600 cm^{-1} range with 5 PLS factors and had a SEC of 0.4 mmol/L, SEP of 0.3 mmol/L, and MPE of 2.2%.

Table 2. RMS noise on 100% lines for first overtone spectra collected from urea calibrators.

Segment, cm^{-1}	6500–6400	6400–6300	6300–6200	6200–6100	6100–6000
RMS noise, μAU	5140	320	58.3	20.5	12.4
Segment, cm^{-1}	6000–5900	5900–5800	5800–5700	5700–5600	5600–5500
RMS noise, μAU	9.3	11.8	36.7	277	1470

SW-NIR SPECTRA

The sw-NIR is a wide spectral region that encompasses numerous high-order combination and overtone vibration transitions. The attraction of this spectral region from an instrument-design standpoint is the availability of inexpensive and robust optical components. From an analytical standpoint, however, the ability to extract high-quality and reliable chemical information from these high-order combination and overtone vibration transitions has not been demonstrated for systems of clinical interest (23). The principal problem stems from the low absorptivity and broadness of these high-order transitions.

The absorbance spectrum of urea over the sw-NIR spectral region reveals a single, broad absorption band. This band is centered at 9925 cm^{-1} with a width at half maximum of 150 cm^{-1} . This wavenumber position and width suggests that this band corresponds to the second-order overtone transitions of both the symmetric and asymmetric N–H stretching vibrations. Although the fundamental bands for these transitions are easily distinguishable at 3350 and 3450 cm^{-1} (20), the broadening effects of high-order transitions results in considerable overlap to the extent that these two bands are no longer resolved.

The ability to measure urea in this spectral region was evaluated by assessing PLS calibration models generated from spectra collected from 79 unique urea calibration solutions. Preparation of these calibration solutions, collection of spectra, splitting of these spectra into calibration and prediction data sets, and analysis of these spectra were performed as described above. Mean values for RMS noise of 100% lines are presented in Table 3. Noise levels were relatively constant across the entire spectral range. This finding is consistent with the low absorptivity of water throughout this spectral range. The measured noise was roughly three- to fivefold higher than the low-noise regions in both the combination and first overtone spectra.

The optimal PLS calibration model corresponded to a 6-factor model over the $10490\text{--}9450 \text{ cm}^{-1}$ spectral range. The results of this model are presented in the concentration correlation plot in Fig. 3. Values for the SEC, SEP, and

MPE were 1.72 mmol/L , 1.28 mmol/L , and 9.5% , respectively. For comparison, the SDC and SDP values were 8.5 and 9.9 mmol/L , respectively, and were considerably greater than the corresponding SEC and SEP values. Both the calibration and prediction data fell along the unity line with no evidence of a systematic bias.

COMPARISON OF SPECTRAL RANGES

A comparison of these three spectral ranges clearly shows that urea is best measured spectroscopically in the combination region. The lack of analytical information in the first overtone precludes this spectral region. Calibration and prediction errors are approximately fourfold larger for models generated from sw-NIR spectra compared with models based on combination spectra. Characteristics that provide sound analytical measurements in the combination region include high spectral quality (low RMS noises) coupled with strong absorption features.

MEASUREMENT OF UREA AND GLUCOSE IN THE DIALYSATE MATRIX

The calibration models described above involve the measurement of urea in a sample matrix where the chemical components of this matrix are essentially constant for each sample. The only variation in samples is the concentration of dissolved urea. This type of experiment demonstrates the sensitivity of the spectroscopic method for measuring urea in the matrix, but the issue of measurement selectivity is not addressed. Selectivity for urea over glucose is examined here as a first step in the evaluation of this measurement scheme for measuring urea selectively in dialysate samples collected during actual dialysis treatments. Glucose is used here because the concentration of glucose in collected dialysate samples is known to vary in accordance with the difference between the concentration of glucose in the patient's blood and in the original dialysate fluid. In practice, glucose is added to the original dialysate solution to avoid hypoglycemia during treatment.

In this experiment, 84 samples were prepared by dissolving solid urea and glucose in the blank dialysate solution. Solutions were designed to provide a random sampling of urea and glucose over a concentration range

Table 3. RMS noise on 100% lines for sw-NIR spectra collected from urea calibrators.

Segment, cm^{-1}	10 400–10 300	10 300–10 200	10 200–10 100	10 100–10 000	10 000–9900
RMS noise, μAU	16.3	16.1	15.7	15.5	15.3
Segment, cm^{-1}	9900–9800	9800–9700	9700–9600	9600–9500	9500–9400
RMS noise, μAU	14.7	15.3	16.3	18.3	22.3

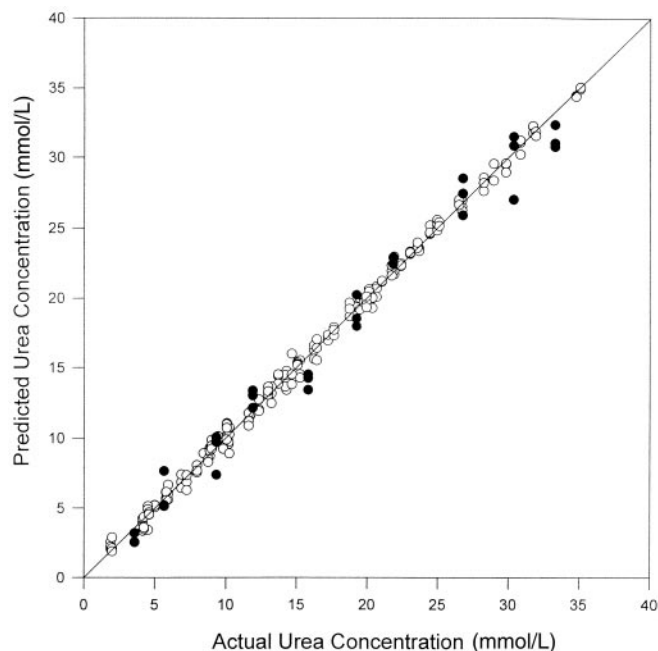


Fig. 3. Concentration correlation plot for urea over the 12 500–8600 cm^{-1} spectral range.

Open circles represent calibration data, and filled circles represent prediction data. The optimum calibration model was built over the 10 490–9450 cm^{-1} range with 6 PLS factors and had a SEC of 1.7 mmol/L, a SEP of 1.3 mmol/L, and a MPE of 9.5%.

of 1–36 mmol/L for each solute. As a result, the concentrations of glucose and urea in the full set of samples lacked any significant correlation. The plot presented in Fig. 4 shows the overall correlation between glucose and urea concentrations in these samples. A linear regression analysis revealed a slope of 0.033 ± 0.059 , a y -intercept of 12.32 ± 1.19 mmol/L, and an r^2 of 0.0012 for these data. The lack of a correlation is critical to assure that the PLS

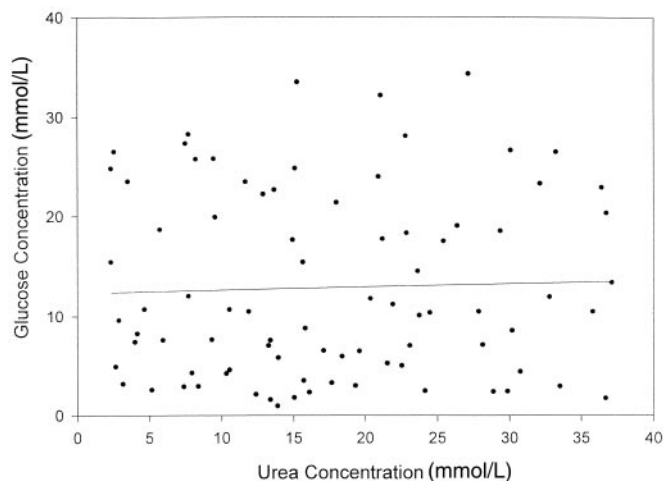


Fig. 4. Correlation plot between urea and glucose in the two component mixtures.

Each data point represents one sample. The line corresponds to a least-squares fit, and the linear regression analysis indicates a slope of 0.033 ± 0.059 , a y -intercept of 12.32 ± 1.19 mmol/L, and an r^2 of 0.0012.

model for urea is based solely on the spectral features of urea with no contribution from glucose. The same procedures detailed above were used for collecting and analyzing the combination spectra collected from these calibration solutions.

The spectral quality for these combination spectra was essentially identical to the combination spectra described above where only urea was added to the solution. Mean values for the RMS noise of 100% lines are summarized in Table 4 for all 84 solutions. From these spectra, the optimized PLS calibration model for urea consisted of a 5-factor model over the 4600–4350 cm^{-1} spectral range. The SEC, SEP, and MPE were 0.6 mmol/L, 0.7 mmol/L, and 7.1% for this calibration model. These values for the SEC and SEP were considerably lower than the corresponding SDC (9.65 mmol/L) and SDP (11.23 mmol/L) for these solutions. The concentration correlation plot in Fig. 5 illustrates the scatter around the unity line. As before, no evidence of a systematic bias is evident in this plot or in the corresponding residual plot (data not shown).

The optimized spectral range for the urea calibration model was significantly different for the two sets of urea calibration solutions. When only urea was varied, the optimized spectral range was 4720–4600 cm^{-1} , which included only the 4650 cm^{-1} urea band. When both urea and glucose concentrations varied, the optimal spectral range shifted to 4600–4350 cm^{-1} , which included only the 4550 cm^{-1} urea band. A potential explanation for this shift in spectral range is the presence of a broad glucose absorption band centered at 4750 cm^{-1} (11). This glucose band strongly overlaps with the 4650 cm^{-1} band of urea, thereby reducing the effectiveness of this urea band for analytical measurements. In contrast, the 4550 cm^{-1} urea band is positioned between the 4750 and 4400 cm^{-1} absorption bands of glucose (11). The overall impact of glucose on the ability to measure urea is an increase in the prediction error by approximately a factor of 2.

One of the attractive features of NIR spectroscopic analysis is the ability to measure multiple species in the sample from a single spectrum. In this experiment, the same spectra were used to generate PLS calibration models for glucose. The optimized result was a 6-factor model over a spectral range of 4450–4300 cm^{-1} . The concentration correlation plot in Fig. 6 presents the results of this model. The SEC, SEP, and MPE were 0.6 mmol/L, 0.4 mmol/L, and 1.7%, respectively. This measurement of glucose appears valid with no evidence of a systematic bias. These findings are essentially identical to those published before for the measurement of glucose in a series of binary solutions where the concentrations of glucose and glutamine are varied randomly within a phosphate–bicarbonate buffer matrix (10). This earlier work reported a 6-factor model over the 4470–4250 cm^{-1} spectral range with a SEC of 0.64 mmol/L, an SEP of 0.41 mmol/L, and a MPE of 2.21%.

Table 4. RMS noise on 100% lines for combination spectra collected from urea/glucose calibrators.

Segment, cm^{-1}	5000–4900	4900–4800	4800–4700	4700–4600	4600–4500
RMS noise, μAU	2280	113	11.0	3.41	2.27
Segment, cm^{-1}	4500–4400	4400–4300	4300–4200	4200–4100	4100–4000
RMS noise, μAU	2.54	6.74	52.8	1007	6120

REAL SAMPLE MEASUREMENTS

We evaluated the selectivity of the proposed method further by attempting to measure urea concentrations in a small set of samples collected during hemodialysis. In this experiment, one sample was collected from five separate dialysis patients at various stages of treatment (early to late in the dialysis process). This collection strategy provided samples that spanned a wide range of urea concentrations (~ 2 – 16 mmol/L). Combination spectra were collected in triplicate for each sample.

Urea concentrations in these samples were predicted from a PLS calibration model that was built from the spectra collected from the urea in dialysate calibration solutions. These same spectra were used to generate the results presented in Table 1 and Fig. 2. The results presented in Fig. 1 and Table 2 were obtained from models generated from single-beam spectra. Single beam spectra could not be used for the analysis of these real samples because these samples, and their corresponding spectra, were collected ~ 1 year after the calibration spectra were obtained. Although these subsequent spectra were collected from the same instrument, considerable

differences (i.e., $\sim 20\%$ difference in the mean single-beam intensity) were noted between the two groups of single-beam spectra. Such differences were expected on the basis of many possible instrumental variations that occurred during the intervening period. Differences in these single-beam spectra were diminished considerably by use of absorbance spectra. The reference spectrum used to compute each absorbance spectrum corresponded to a urea-free aliquot of the dialysate solution. For the calibration spectra, a reference spectrum was collected at the beginning of each day during the experiment. For the real samples, a single reference spectrum was collected at the beginning of the data collection session. In both cases, absorbance spectra were computed using the most recently collected reference spectrum.

The optimized parameters described above for this calibration data set were used to generate the PLS calibration model. Specifically, the entire set of spectra from all calibration solutions was used to build a 5-factor calibration model over the 4720 – 4600 cm^{-1} spectral range. This model was then used to predict the concentration of urea in each of the five actual dialysate samples. The results of

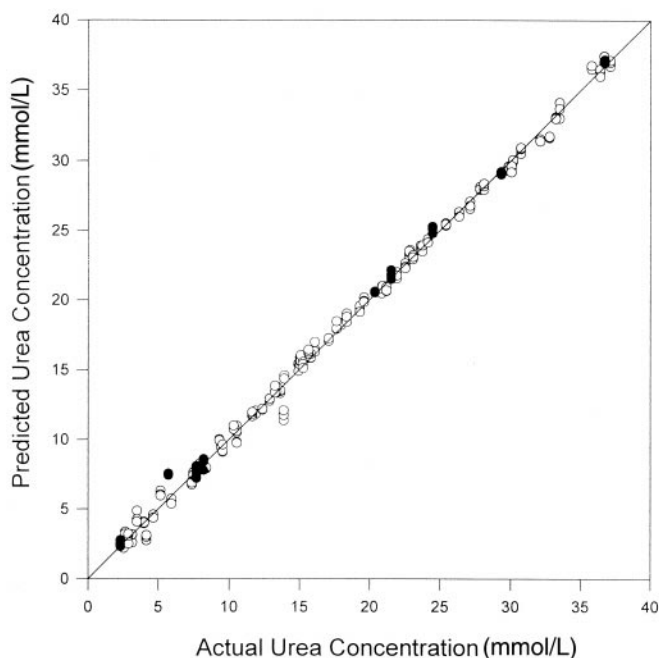


Fig. 5. Concentration correlation plot for urea in the two component mixtures.

Open circles represent calibration data, and filled circles represent prediction data. The optimum calibration model for urea was built over the 4600 – 4350 cm^{-1} spectral range with 5 PLS factors and a SEC of 0.6 mmol/L, a SEP of 0.7 mmol/L, and a MPE of 7.1% .

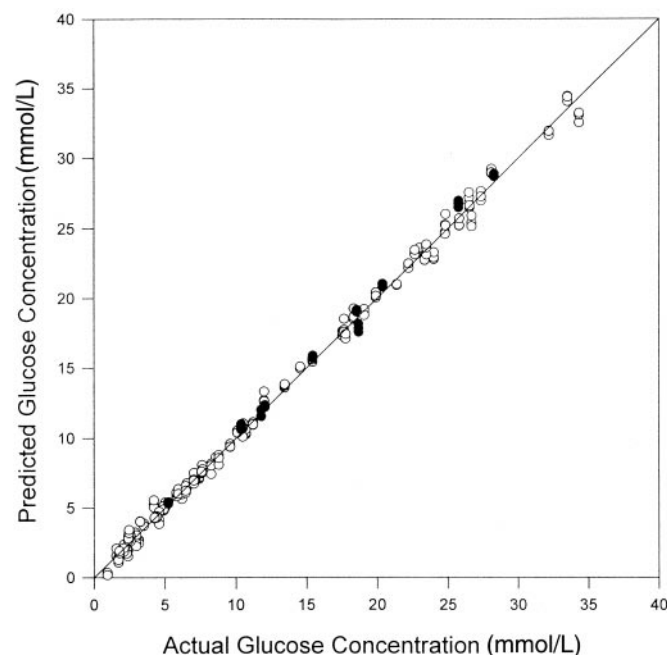


Fig. 6. Concentration correlation plot for glucose in the two component mixtures.

Open circles represent calibration data, and closed circles represent prediction data. The optimum calibration model was built over the 4450 – 4300 cm^{-1} spectral range with 6 PLS factors, a SEC of 0.6 mmol/L, a SEP of 0.4 mmol/L, and a MPE of 1.7% .

Table 5. Urea measurements in real dialysate samples.

Sample no.	Reference urea concentration, ^a mmol/L	NIR-predicted urea concentration, ^b mmol/L	Absolute error, ^b mmol/L	Relative error, ^b %
1	15.67	15.18	0.49	3.14
2	3.88	4.13	0.25	6.48
3	10.73	10.70	0.03	0.24
4	6.29	6.03	0.26	4.21
5	1.98	1.93	0.05	2.41

^a Determined by the urease/Berthelot reaction scheme (18).

^b Average of three measurements.

this analysis are summarized in Table 5 for each sample. Cumulatively, the SEP was 0.29 mmol/L and the MPE was 3.8%. This cumulative prediction error for the real samples was remarkably similar to the SEP reported above for this calibration data set. This finding indicates that the chemical matrix of these real samples does not interfere with the urea measurement. In addition, these successful predictions are noteworthy considering that calibration spectra were collected 1 year before the analysis spectra.

Discussion

NIR spectroscopy can be used to measure urea selectively within the chemical matrix of the hemodialysis dialysate fluid. The best analytical performance is obtained using spectra collected over the combination spectral range (5000–4000 cm^{-1}). Prediction errors on the order of 0.3 mmol/L are possible when the spectral quality is on the order of 2–3 μAU for solutions with an optical pathlength of 1.5 mm. The addition of varying concentrations of glucose within the dialysate matrix degrades the prediction performance by a factor of 2. Nevertheless, selective urea measurements are possible in solutions with glucose variations of 1–35 mmol/L. A calibration model based on prepared dialysate samples was used to measure urea in real hemodialysis dialysate samples with prediction errors on the same order as those for urea in prepared samples.

These findings support our objective to measure urea noninvasively as a means to follow in real-time the collection of urea in the recipient dialysate stream. Future research will expand the number of real hemodialysis dialysate samples to assess the accuracy of a noninvasive NIR measurement of urea in samples collected during actual hemodialysis treatments.

The contributions and guidance provided by Professor Michael Flanigan are greatly appreciated. This work was sponsored by a grant from the National Institutes of Diabetes and Digestive and Kidney Diseases (DK-45126).

References

- Levin NW. Adequacy of dialysis. *Am J Kidney Dis* 1994;24:308–15.
- Sombolos K, Natse T, Zoumaridis N, Mavromatidis K, Karagianni A, Scandalos J, Fitili C. Urea concentration gradients during conventional hemodialysis. *Am J Kidney Dis* 1996;27:673–9.
- Keen M, Schulman G. Current standards for dialysis adequacy. *Adv Ren Replace Ther* 1995;2:287–94.
- Gerrad LJ, Canaud BC, McCready WG. Optimal hemodialysis—the role of quantification. *Semin Dial* 1994;7:236–45.
- Shohat J, Boner G. Adequacy of hemodialysis 1996. *Nephron* 1997;76:1–6.
- Klein E, Montalvo JG, Wawro R, Holland FF, Lebeouf A. Continuous monitoring of urea levels during hemodialysis. *Int J Artif Organs* 1978;1:116–22.
- Keshaviah PR, Ebben JP, Emerson PF. On-line monitoring of the delivery of the hemodialysis prescription. *Pediatr Nephrol* 1995; 9:S2–8.
- Zamponi S, Cicero BL, Mascini M, Ciana LD, Sacco S. Urea solid-state biosensor suitable for continuous dialysis control. *Talanta* 1996;43:1373–7.
- Jacobs P, Sansen W, Homrouckx R. Continuous monitoring of the spent dialysate urea level using a disposable biosensor. *ASAIO J* 1994;40:M393–400.
- Chung H, Arnold MA, Rhie M, Murhammer, DW. Simultaneous measurement of glucose and glutamine in aqueous solutions by near infrared spectroscopy. *Appl Biochem Biotechnol* 1995;50: 109–25.
- Riley MR, Rhie M, Zhou X, Arnold MA, Murhammer DW. Simultaneous measurement of glucose and glutamine in insect cell culture media by near infrared spectroscopy. *Biotechnol Bioeng* 1997;55:11–5.
- Hazen KH, Arnold MA, Small GW. Measurement of glucose and other analytes in undiluted human serum with near-infrared transmission spectroscopy. *Anal Chim Acta* 1998;371:255–67.
- Burmeister JJ, Arnold MA. Evaluation of measurement sites for noninvasive blood glucose sensing with near-infrared transmission spectroscopy. *Clin Chem* 1999;45:1621–7.
- Marbach R, Koschinsky T, Gries F, Heise H. Noninvasive blood glucose assay by near-infrared diffuse reflectance spectroscopy of the human inner lip. *Appl Spectrosc* 1993;47:875–81.
- Arnold MA, Burmeister J, Small G. Phantom glucose calibration models from simulated noninvasive human near-infrared spectra. *Anal Chem* 1998;70:1773–81.
- Thomas EV. A primer on multivariate calibration. *Anal Chem* 1994;66:795A–804A.
- Kramer R. Chemometric techniques for quantitative analysis. New York: Marcel Dekker, Inc., 1998:195pp.
- Ngo TT, Phan APH, Yam CF, Lenhoff, HM. Interference in the determination of ammonia with the hypochlorite-alkaline phenol method of Berthelot. *Anal Chem* 1982;54:46–9.
- Silverstein RM, Bassler GC, Morrill TC, eds. Spectrometric identification of organic compounds, 5th ed. New York: Wiley & Sons, 1991:122.
- Pouchert, CJ, ed. The Aldrich library of FT-IR spectra, 2nd ed. Milwaukee, WI: Aldrich, 1997:1306D.
- Edward, SK, Mahpour, M. The identification and origin of N–H overtone and combination bands in the near-infrared spectra of simple primary and secondary amides. *Spectrochim Acta A* 1973; 29:1233–46.
- Hazen KH, Arnold MA, Small GW. Measurement of glucose in water with first-overtone near-infrared spectra. *Appl Spectrosc* 1998;52:1597–605.
- Khalil, OS. Spectroscopic and clinical aspects of noninvasive glucose measurements. *Clin Chem* 1999;45:165–77.